

# Hydrolysis of Cellobiose over Selective and Stable Sulfonated Activated Carbon Catalysts

Guo Shiou Foo,<sup>†</sup> Adam H. Van Pelt,<sup>†</sup> Daniel Krötschel,<sup>†</sup> Benjamin F. Sauk,<sup>†</sup> Allyson K. Rogers,<sup>†,‡</sup> Cayla R. Jolly,<sup>†</sup> Matthew M. Yung,<sup>‡</sup> and Carsten Sievers<sup>\*,†</sup>

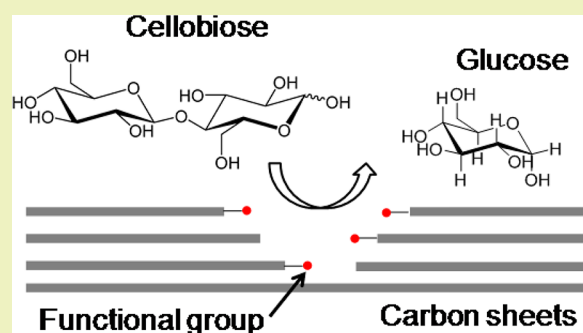
<sup>†</sup>School of Chemical & Biomolecular Engineering, Georgia Institute of Technology, 311 Ferst Drive NW, Atlanta, Georgia 30332, United States

<sup>‡</sup>National Renewable Energy Laboratory, 1617 Cole Boulevard, Golden, Colorado 80401-3305, United States

## S Supporting Information

**ABSTRACT:** Activated carbon is functionalized by different treatments with sulfuric acid and hot liquid water and used as catalyst for the hydrolysis of cellobiose in a continuously operated fixed bed reactor. Characterization results reveal that the chemically treated materials are more disordered with a lower degree of graphitization, while adsorption isotherms demonstrate that van der Waals forces dominate the interaction between carbohydrates and the surface of catalysts. All catalysts are stable during the hydrolysis of cellobiose under flow conditions. Carbon catalysts with a limited fraction of sulfonic acid groups exhibit moderate cellobiose conversion but a higher and sustained glucose selectivity. The high selectivity is attributed to a higher fraction of weak acid sites, where degradation of glucose only occurs to a limited extent due to less accessibility and competitive adsorption with cellobiose. Furthermore, the strong sulfonic acid groups are more accessible for degradation reactions to occur. In contrast, the catalyst with a higher fraction of sulfonic acid groups shows increased cellobiose conversion but decreased glucose selectivity because glucose monomers can be converted to degradation products at these sites.

**KEYWORDS:** Glucose, Solid acid, Defect sites, Degradation, Fixed bed reactor



## INTRODUCTION

Biomass is an important and renewable feedstock for the sustainable production of chemicals, fuels, and energy.<sup>1</sup> In particular, the depolymerization of biomass-derived polymers into monomers is crucial for its subsequent conversion into valuable chemicals.<sup>2</sup> The most abundant polymer in most types of biomass is cellulose. Cellulose is a recalcitrant material that is composed of glucose monomers linked by  $\beta$ -1,4-glycosidic bonds.<sup>3</sup> Hydrolysis of cellulose is an attractive method to produce glucose as a useful platform chemical that can be converted to 5-hydroxymethylfurfural (HMF) and levulinic acid using solid acid catalysts.<sup>4</sup> It was also reported that glucose can be converted to lactic acid and gluconic acid using supported metal catalysts in an alkaline solution.<sup>5</sup> Gluconic acid is used in the food and pharmaceutical industries. Additionally, the isomerization of glucose to fructose can be carried out over Lewis acidic zeolites followed by conversion to other useful products.<sup>6</sup> Furthermore, glucose can be fermented to obtain other important products such as succinic acid, 3-hydroxy propionic acid, itaconic acid, and glutamic acid.<sup>7</sup>

Enzymatic hydrolysis has received the most attention among the strategies for hydrolyzing cellulose to glucose.<sup>8</sup> However, the recalcitrance of feedstocks and the relatively low rates of such enzymatic reactions have limited the commercial potential

of this approach. Cellulose can be hydrolyzed more rapidly using near critical or supercritical water<sup>9,10</sup> or strong Brønsted acid catalysts such as sulfuric acid, which are able to decompose the hydrogen bonds between the polymeric chains and the  $\beta$ -1,4-glycosidic bonds between the glucose monomers.<sup>11–14</sup> However, such processes suffer from the formation of degradation products when the glucose remains exposed to the reaction medium, and costly separation of the homogeneous reaction mixture is needed. To a certain extent, the formation of degradation products can be reduced by limiting the residence time of the products in the reactor, but a certain part of the feedstock will be incompletely hydrolyzed to oligosaccharides if this strategy is applied.<sup>14,15</sup> Therefore, efforts have to be targeted toward increasing the yield of glucose so that the efficiency of these processes can be maximized.

It has been reported that sulfonated carbon is an effective and reusable catalyst for the hydrolysis of cellulose and cellobiose.<sup>16–22</sup> However, most of these studies were performed using batch reactors. Studies using heterogeneous catalysts in flow reactors are needed to determine the feasibility

**Received:** February 15, 2015

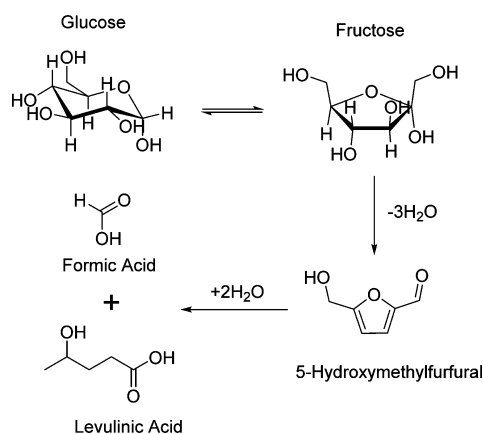
**Revised:** July 20, 2015

**Published:** July 23, 2015

of such a process on a large scale, at which flow reactors are expected to provide favorable process economics and improvements in yields.<sup>23</sup> Interestingly, weak acid sites on carbon such as carboxylic acid and phenol groups can also be active in the hydrolysis of carbohydrates.<sup>15,24</sup> The reaction could even be induced by forced interactions between glycosidic oxygen atoms in glucan chains and weakly acidic hydroxyl groups on silica and alumina.<sup>25–27</sup> We recently showed that there is a substantial loss in total acid sites when sulfonated activated carbon is treated in hot liquid water between 150 and 225 °C, but the remaining surface functional groups after 12 h of treatment are stable.<sup>28</sup> In addition, it was demonstrated that these stable functional groups in synergy with defect sites created in the acidification process are effective sites for the hydrolysis of cellulose.<sup>29</sup> We rationalized that the adsorption of glucan chains on defect sites or the edges of the graphene sheets induces a conformational change of the glucan that allows an in-plane functional group of the catalyst to attack the exposed glycosidic bond. This enables even weak acid sites to participate in the hydrolysis reaction.<sup>3</sup>

However, a conundrum exists where acidification with sulfuric acid creates the needed defect sites but also imparts strongly acidic sulfonic acid groups on carbon. It is hypothesized that these strong acid sites may favor degradation reactions and, thus, have a negative impact on glucose yield in hydrolysis reactions. Scheme 1 shows a typical degradation

**Scheme 1. Reaction Pathway for the Degradation of Glucose**



pathway for glucose. Cellobiose is the disaccharide of glucose and can be considered as a representative model compound for glucose oligomers. By studying the hydrolysis of cellobiose in a well-defined feed stream, it is possible to gain insight into the impact of sulfonic acid groups in hydrolysis.

In this study, sulfonated activated carbon catalysts with different fractions of sulfonic acid groups are synthesized and characterized by various physicochemical techniques. The catalysts are used for the hydrolysis of cellobiose in a continuous reactor. The combination of the results from these experiments provides valuable structure–property relationships. The results of this study will help to identify the ideal strength of acid sites for the hydrolysis of carbohydrates.

## EXPERIMENTAL SECTION

**Materials.** Activated charcoal (untreated, granular, 4–8 mesh, made from peat bog), sulfuric acid (95.0–98.0%), glucose (>99.5%), cellobiose (>98%), sodium hydroxide (>98%, pellets), potassium

hydrogen phthalate (>99.95%), sodium carbonate (>99%), sodium bicarbonate (>99.7%), and potassium bromide (FTIR grade, >99%) were purchased from Sigma-Aldrich. Deionized water was further purified using a Barnstead NANOpure ultrapure water system to 18.2 MΩ/cm.

**Catalyst Preparation.** The activated charcoal was used as received. To acidify the catalyst, 8.0 g of untreated carbon was mixed with 80 mL of sulfuric acid (10 M) at 100 °C for 30 min. The suspension was filtered and washed with deionized (DI) water until the filtrate had a neutral pH. To ensure that only stable functional groups are present,<sup>28</sup> the sample was treated in hot liquid water at 200 °C and autogenic pressure for 24 h. The sample was filtered and washed with DI water again until the filtrate had a neutral pH. This sample was named acidified carbon. The catalyst that has undergone acidification and hot water treatment twice was named reacidified carbon. For the fourth sample, as-received carbon was initially treated in hot liquid water at 200 °C for 24 h and subsequently subjected to the same acidification and hot water treatment as the other samples. The sample is named hot water treated (HWT) acidified carbon.

**Raman Spectroscopy.** To probe the disordered carbon materials, Raman spectra were collected on a Confocal Raman Microscope Alpa-Witek with a laser wavelength of 514 nm. Each sample was placed across a glass slide. For each spectrum, 10 scans were recorded, and three spectra were obtained for each sample at different locations. Peak fitting was performed with the GRAMS/AI software.

**X-ray Diffraction (XRD).** Powder XRD patterns were measured on a Philips X'pert diffractometer equipped with an X'celerator module using Cu Kα radiation. Diffractograms were collected at incident angles from 2θ = 5 to 70° at a step size of 0.0167°.

**NMR Spectroscopy.** <sup>13</sup>C direct polarization (DP) magic angle spinning (MAS) NMR spectra were recorded on a Bruker DSSX 300 spectrometer. The samples were loaded into a 4 mm zirconia rotor and spun at a frequency of 10 kHz. Adamantane was used as a reference material, and the peak at δ = 38.45 ppm was set as the reference. The resonance frequency of <sup>1</sup>H is 300.2 MHz and that of <sup>13</sup>C is 75.5 MHz. High power <sup>1</sup>H decoupling was used during the sampling of the <sup>13</sup>C magnetization. A π/2 pulse (5 μs) was applied, while the recycle delay was 4 s. Each spectrum was accumulated with about 20,000 scans.

**Nitrogen and Carbon Dioxide Physisorption.** N<sub>2</sub> and CO<sub>2</sub> physisorption measurements were carried out with a Micromeritics ASAP 2020 physisorption analyzer at 77 and 273 K, respectively. Prior to analysis, ca. 150 mg of each sample was evacuated in vacuum for 4 h at 150 °C. For nitrogen physisorption, the surface area and pore volumes were calculated using the BET method<sup>30</sup> and the BJH method,<sup>31</sup> respectively. For carbon dioxide physisorption, the pore volume was calculated by using the DFT method.<sup>32</sup>

**Elemental Analysis.** All carbon samples were sent to Atlantic Microlab for elemental analysis to determine their sulfur contents. The samples were also sent to Elemental Analysis, Inc. for proton induced X-ray emission (PIXE) analysis to determine the amount of inorganic species present.

**Boehm Titration.** The type and concentration of functional groups present on the carbon materials were determined by Boehm titration. This was performed by following the procedures as reported in the literature.<sup>28,29,33,34</sup> In short, 1.5 g of each sample was added to 50 mL of aqueous solutions of NaOH, NaHCO<sub>3</sub>, and Na<sub>2</sub>CO<sub>3</sub>. The concentration of each base solution was 0.05 M. The slurries were shaken for a total of 24 h and filtered, and aliquots of the filtrate (10 mL) were collected. For the aqueous NaHCO<sub>3</sub> and NaOH solutions, 20 mL of 0.05 M HCl<sub>aq</sub> was added. For the aqueous Na<sub>2</sub>CO<sub>3</sub> solution, 30 mL of 0.05 M of HCl<sub>aq</sub> was added. The solutions were outgassed with N<sub>2</sub> for 2 h and back-titrated with 0.05 M solution of NaOH until an end point (pH 7.0) was reached. The calculated standard deviations are 6 μmol/g, 10 μmol/g, and 10 μmol/g for the carboxylic acid group, lactonic group, and phenolic group, respectively.

**Hydrolysis of Cellobiose.** Hydrolysis of cellobiose (0.03 M) was performed in a fixed bed down-flow reactor (0.635 cm outer diameter Swagelok stainless steel tube). Quartz wool was used at both ends of the reactor to keep the catalyst bed in place. The reactor temperature was set at 200 °C, and the pressure was controlled at 25 bar with the

use of an Equilibar EB1LF2 back pressure regulator with a PTFE/glass diaphragm. The cellobiose feed (0.03 M) was supplied from a 1 L glass bottle using an Agilent 1100 Series HPLC pump at a flow rate of 0.5 mL/min. The reaction products were collected every 20 min using a Valco selector valve for HPLC analysis. The catalysts were tested at various residence times. The cellobiose feed was initially pumped at a flow rate of 0.5 mL/min for 3.5 h. Then, the flow rate was increased to 0.75 mL/min for another 3.5 h and 1.00 mL/min for another 3.5 h. For these tests, the reaction products were collected every 30 min. An additional experiment was performed with an aqueous glucose solution (0.03 M) as feed. The analysis of reaction products was performed using an Agilent 1260 Infinity HPLC with a Grace Davison Prevail carbohydrate column. The concentration of the sugar molecules was measured using a refractive index detector (RID). A five-point calibration curve was used to determine the concentration of cellobiose and glucose. With the available HPLC analysis setup, only glucose and fructose were detected as products analytically from the conversion of cellobiose and glucose, respectively. Thus, the carbon balance could not be closed. The weight to feed ratio (W/F), expressed in  $\text{g} (\text{mmol h}^{-1})^{-1}$ , is defined as the ratio between the mass of the catalyst (g) and the molar feed rate of the reactant ( $\text{mmol h}^{-1}$ ). All of the reactivity experiments were carried out under conditions free of mass transfer limitations (see Supporting Information).

**Adsorption Isotherms.** Standard glucose solutions of various concentrations (0.05 to 0.6 M) were prepared. Standard cellobiose solutions of various concentrations (0.01 to 0.12 M) were also prepared. Preweighed amounts of the carbon sample (ca. 80 mg) were mixed with each sugar solution (1.000 mL) in 1.5 mL microcentrifuge tubes, mixed using a vortexer for 30 s, and placed on a shaker table for 24 h. Subsequently, the slurries were centrifuged (10 min) at 10,000 rcf. The supernatant was removed and analyzed using an Agilent 1260 Infinity HPLC with a Grace Davison Prevail Carbohydrate ES column. To determine the concentration of the sugar molecules, a RID was used. The mobile phase used consisted of 75 vol % acetonitrile and 25 vol % water. The flow rate and injection volume were 1.0 mL/min and 0.6  $\mu\text{L}$ , respectively. The uptake was calculated with  $q = (V(C_0 - C_e))/m_{\text{cat}}$  where  $q$  and  $V$  are the specific uptake (mol/g) and volume of sugar solution used (L), respectively.  $C_0$  and  $C_e$  are the initial and equilibrium concentrations (mol/L) of the sugar solution, respectively, and  $m_{\text{cat}}$  is the mass of carbon sample used (g). For each molecule, three isotherms were obtained for each adsorbent. The Langmuir isotherm parameters were determined via linear regression for each isotherm.<sup>29</sup>

## RESULTS

The Raman spectra of the treated carbon materials had two sharp peaks, the D band around  $1350 \text{ cm}^{-1}$  and the G band around  $1600 \text{ cm}^{-1}$  (Figure S3A). These two bands are usually assigned as the  $A_{1g}$  and  $E_{2g}$  mode, respectively.<sup>37</sup> A broad and intense peak due to amorphous  $\text{sp}^3$  carbon was not observed at  $500 \text{ cm}^{-1}$ , indicating that the species is not present to a large extent.<sup>38</sup> The two complex D and G bands can be deconvoluted into five components at  $1208 \text{ cm}^{-1}$ ,  $1352 \text{ cm}^{-1}$ ,  $1529 \text{ cm}^{-1}$ ,  $1572 \text{ cm}^{-1}$ , and  $1598 \text{ cm}^{-1}$  (Figure S3B). These peaks are assigned as polyenes (D4), graphene edges (D1), amorphous carbon (D3), graphitic carbon (G), and graphene sheets (D2), respectively.<sup>39</sup> After deconvolution, the parameter  $I_{D1}/(I_G + I_{D1} + I_{D2})$  can be used to gauge the degree of graphitization of the carbon materials, where  $I$  is the integral of the fitted peak.<sup>40</sup> As-received carbon displayed the highest degree of graphitization, indicating that it had the most organized structure (Table 1). After treatment with sulfuric acid, the degree of graphitization of the treated carbon samples was reduced. The  $I_{D1}/(I_G + I_{D1} + I_{D2})$  values for the treated samples were within the standard deviation of 0.006. The coefficient of determination ( $R^2$  value) for the deconvolution of individual spectra was greater than 0.99 for each spectrum.

**Table 1. Degree of Graphitization of Carbon Catalysts**

catalyst	$I_{D1}/(I_{D1} + I_G + I_{D2})$
as-received	0.745
acidified carbon	0.716
HWT acidified carbon	0.716
reacidified carbon	0.710

XRD patterns of all the carbon catalysts displayed two broad peaks at  $2\theta$  angles of  $24^\circ$  and  $42^\circ$  (Figure S4). These are assigned as the (002) and (100) or (101) planes of graphite crystallites, respectively.<sup>41,42</sup> A small, sharp peak at  $26.6^\circ$  is also observed for all of the samples, and it is assigned to diffraction at the (002) plane of graphite-like carbon.<sup>43,44</sup> This demonstrates that treatment with hot liquid water and sulfuric acid did not affect the limited crystallinity of the carbon structure to a measurable extent.

$^{13}\text{C}$  DP MAS NMR spectra of the carbon materials exhibited a broad and intense peak at 119 ppm (Figure S5). This is assigned as the nonprotonated core carbon in the polyaromatic structure.<sup>45,46</sup> The broad peak also contained contributions from other species such as exterior carbon in different environments, illustrating that the network of activated carbon is highly complex. The low intensity of aliphatic carbon between 0 and 40 ppm also suggests that most of the carbon in the structure is polyaromatic and  $\text{sp}^2$ -hybridized. The high similarity of the spectra of different samples indicates that acidification does not change the hybridization of a significant fraction of the carbon species in the sample.

The pore size distributions of the carbon catalysts obtained by  $\text{CO}_2$  and  $\text{N}_2$  physisorption are shown in Figure 1. In the

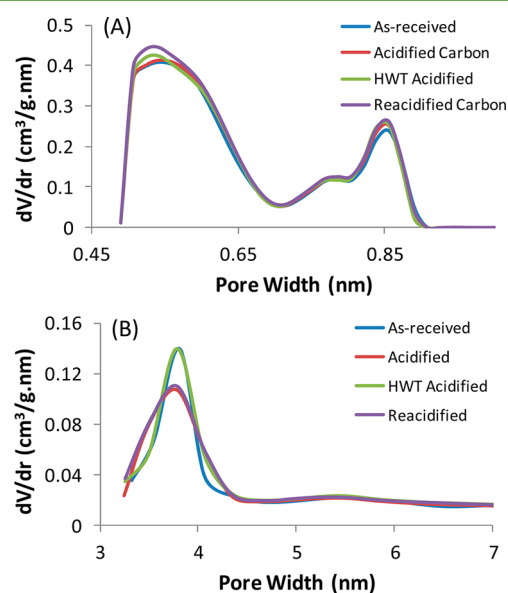


**Figure 1.** Pore size distribution of carbon catalysts (A) 0.45 to 1.00 nm determined by  $\text{CO}_2$  physisorption and (B) 3 to 6 nm determined by  $\text{N}_2$  physisorption.

microporous range, the pore size distributions of the materials were similar (Figure 1A). However, in the mesoporous range, HWT acidified carbon had almost the same pore size distribution compared to that of the as-received carbon (Figure 1B). Acidified carbon and reacidified carbon had a lower contribution of pores that were around 3.8 nm in size. The surface area of the materials remained unchanged in both the



**Table 2. Surface Properties and Reactivity of Carbon Catalysts in the Hydrolysis of Cellobiose<sup>a</sup>**

catalyst	surface area (m <sup>2</sup> /g) <sup>b</sup>	total acid sites (μmol/g) <sup>c</sup>	sulfonic groups (μmol/g) <sup>d</sup>	fraction of sulfonic groups	conversion (%) <sup>e</sup>	glucose selectivity (%) <sup>e</sup>
no catalyst					21	40
as-received carbon	623	129			21	43
acidified carbon	620	403	169	0.42	50	42
HWT acidified carbon	633	510	134	0.26	41	63
reacidified carbon	654	544	91	0.17	40	60

<sup>a</sup>200 °C, 25 bar, 100 mg catalyst, 0.5 mL/min of 0.03 M cellobiose solution. <sup>b</sup>Determined by N<sub>2</sub> physisorption. <sup>c</sup>Determined by Boehm titration. <sup>d</sup>Determined by elemental analysis. <sup>e</sup>Determined by HPLC analysis.

microporous and mesoporous range (Table S2). The BET surface area of the carbon catalyst did not change significantly after treatment with sulfuric acid and hot liquid water (Table 2).

PIXE analysis of the carbon materials was performed to determine the amounts of different inorganic species in the catalysts that could affect hydrolysis and side reactions. As-received carbon had 0.1 to 0.5 wt % of sodium, magnesium, aluminum, silicon, sulfur, calcium, and iron (Table S3). The contents of other inorganic species were small. During acidification with sulfuric acid, the content of all inorganic elements in the chemically treated carbons were reduced significantly, except for sulfur, which is due to the formation of sulfonic acid groups.

Boehm titration revealed that as-received carbon had a low concentration of acid sites before acidification (Table 2). Even though PIXE analysis revealed that untreated carbon contained 0.16 wt % of sulfur, it was reported that these sulfur species are highly oxidized and that they can be attributed to metal sulfates or sulfonic esters.<sup>28</sup> Treatment with sulfuric acid removes these species, and the sulfur content of the treated samples can be attributed to the presence of sulfonic acid groups. Therefore, the as-received carbon did not contain sulfonic acid groups (Table 2). The carbon materials that had been subjected to chemical treatment had increased concentrations of acid sites. Besides sulfonic acid groups, weaker acid sites such as phenol, lactone, and carboxylic acid groups were also present (Table S4). Acidified carbon had the highest fraction of sulfonic acid groups, followed by HWT acidified carbon and reacidified carbon.

The hydrolysis of cellobiose over different carbon catalysts was studied using a continuously operated fixed bed reactor (Figure S6). Over the course of 4 h on stream, the values of conversion and glucose selectivity were always within 10% of the average value, and the fluctuation appeared to be random. This indicates that the carbon catalysts are stable during the hydrolysis reaction.<sup>28</sup> As-received carbon gave a conversion and glucose selectivity of 21% and 43%, respectively (Table 2). These values are close to the ones obtained in the absence of a catalyst. Acidified carbon displayed the highest conversion but lowest glucose selectivity compared to those of the rest of the catalysts (Figure S6). Its average conversion and glucose selectivity were 50% and 42%, respectively (Table 2). HWT acidified carbon and reacidified carbon provided lower conversions but the highest selectivities.

Since HWT acidified carbon and reacidified carbon have similar reactivity, acidified carbon and HWT acidified carbon were further tested at various W/F ratios under the same reaction conditions of 200 °C and 25 bar. Figure 2 shows the conversion and glucose selectivity over the carbon catalysts. As the W/F ratio decreased, the steady state conversion over both

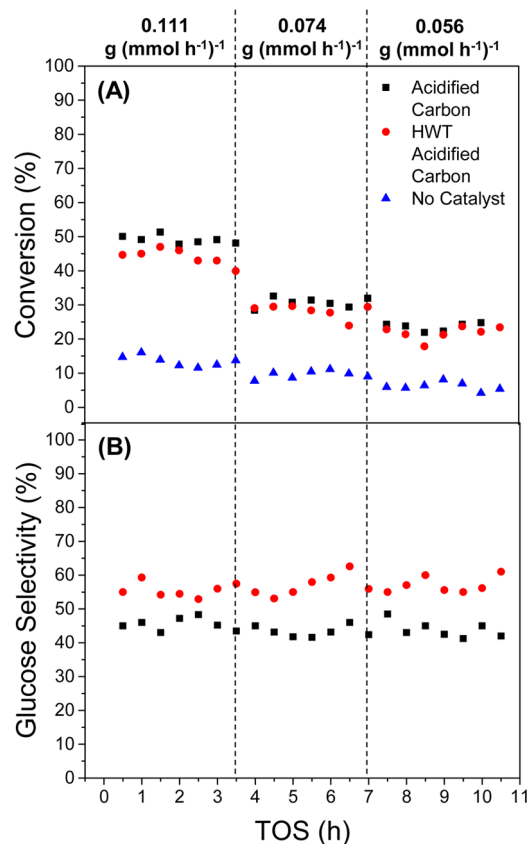


**Figure 2.** (A) Conversion and (B) glucose selectivity of cellobiose hydrolysis at various W/F ratios using acidified carbon, HWT acidified carbon, and an empty reactor. Reaction conditions: 200 °C, 25 bar, 0.03 M cellobiose in water, and 100 mg catalyst.

catalysts decreased. Acidified carbon had a slightly higher conversion compared to that of HWT acidified carbon at all W/F values. However, both catalysts had a constant glucose selectivity with increasing time on stream. Acidified carbon had an average glucose selectivity of 43%, while HWT acidified carbon had an average glucose selectivity of 59%. The glucose selectivity of the reaction without catalyst is not shown because of the high error margin associated with the low glucose concentration in the product stream.

To further study the reason for differences in glucose selectivity over different catalysts, an aqueous glucose solution (0.03M) was fed into the fixed bed reactor setup under the same reaction conditions. Figure 3 shows the conversion of glucose over acidified carbon and HWT acidified carbon. For both catalysts, glucose conversion decreased with decreasing W/F ratio, and acidified carbon had a higher steady state conversion at all W/F ratios. However, conversion was low for

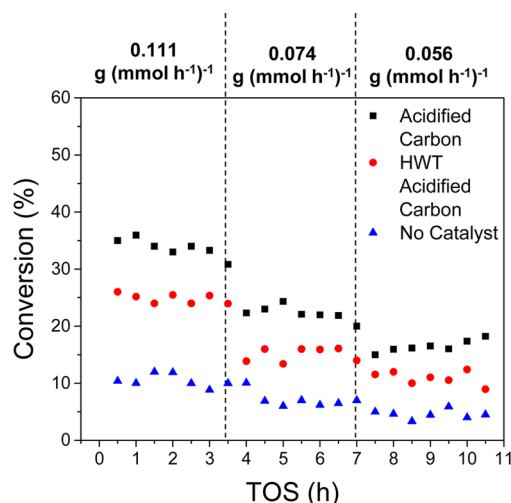


**Figure 3.** Conversion of glucose over acidified carbon, HWT acidified carbon, and in an empty reactor at various W/F ratios. Reaction conditions: 200 °C, 25 bar, 0.03 M glucose in water, and 100 mg catalyst.

the reaction in the absence of a catalyst. Only fructose was identified as a product using HPLC analysis, and its selectivity is shown in Figure S7.

Table 3 shows the apparent rate constants that are calculated based on the conversion of cellobiose and glucose in

**Table 3.** Apparent Rate Constants for the Conversion of Cellobiose ( $k_{CB}$ ) and Glucose ( $k_{Glu}$ ) in an Empty Reactor ( $s^{-1}$ ) and Using Carbon Catalysts ( $L/g_{cat}\cdot s$ )

catalyst	rate constants		$k_{CB}/k_{Glu}$
	$k_{CB}$	$k_{Glu}$	
no catalyst	$(5.6 \pm 0.5) \times 10^{-4}$	$(4.1 \pm 0.1) \times 10^{-4}$	1.37
acidified carbon	$(3.7 \pm 0.2) \times 10^{-5}$	$(2.4 \pm 0.2) \times 10^{-5}$	1.55
HWT acidified carbon	$(3.5 \pm 0.2) \times 10^{-5}$	$(1.7 \pm 0.1) \times 10^{-5}$	2.05

Figures 2 and 3. For all reactions, the reaction rate constants for cellobiose conversion were higher than those for glucose conversion. However, the ratio of  $k_{CB}$  to  $k_{Glu}$  was higher in the presence of the catalysts, especially, HWT acidified carbon.

Adsorption isotherms of glucose and cellobiose on the carbon materials were obtained to understand the effect of functional groups and defect sites on the adsorption of oligomers. Table 4 shows the Langmuir adsorption constants obtained by linear regression. An example of adsorption isotherms of glucose and cellobiose on as-received carbon is shown in Figure S8. The maximum uptake of each adsorbent was normalized by its surface area for easier comparison. Adsorption coefficients had a standard deviation of 30%. The adsorption coefficient ( $K$ ) obtained for glucose on untreated carbon was 37 L/mol, while  $K$  increased significantly when cellobiose was used as the sorbate. The adsorption coefficients for glucose and cellobiose on the acidified materials were significantly lower than the corresponding values for as-received carbon. Specifically, the decrease was ca. 60% for glucose and ca. 40% for cellobiose.  $K$  was similar in value for all of the chemically treated carbon materials. The difference in free energy ( $\Delta\Delta G$ ) between cellobiose and glucose for as-received carbon was  $-1.78$  kcal/mol. After they were treated with sulfuric acid, the carbon materials had lower  $\Delta\Delta G$  values. As-

**Table 4.** Langmuir Adsorption Constants of Glucose and Cellobiose on Carbon Catalysts<sup>a</sup>

adsorbent	glucose		cellobiose		$\Delta\Delta G$ (kcal/mol)
	normalized $q_m$ (mg/m <sup>2</sup> )	$K$ (L/mol)	normalized $q_m$ (mg/m <sup>2</sup> )	$K$ (L/mol)	
as-received carbon	0.135	37	0.171	650	$-1.78$
acidified carbon	0.190	11	0.163	352	$-2.06$
HWT acidified carbon	0.196	10	0.189	415	$-2.24$
reacidified carbon	0.200	14	0.177	377	$-2.01$

<sup>a</sup> $q_m$ : maximum uptake (mg/g).  $K$ : adsorption coefficient.

received carbon had a normalized maximum uptake ( $q_m$ ) of 0.135 mg/m<sup>2</sup> and 0.171 mg/m<sup>2</sup> for glucose and cellobiose, respectively. The treated samples had higher values of  $q_m$  for the adsorption of glucose, but the values were not significantly different for the adsorption of cellobiose compared to that of as-received carbon.

## DISCUSSION

**Structure of Carbon Catalysts.** Carbon based materials are increasingly used in heterogeneous catalysis with applications toward the production of fine chemicals.<sup>21</sup> Additionally, they are widely used as adsorbents and separation media.<sup>47</sup> For these applications, the performance is largely determined by the morphology and surface chemistry of the carbon material. An in-depth understanding of the structure of carbon catalysts is required so that its properties can be related to its hydrolysis activity. XRD results show that treatment with sulfuric acid and hot liquid water did not affect the low crystallinity of the graphite crystallites to a measurable extent. Furthermore, the diffraction peaks are attributed to the stacking of carbon sheets (Figure S4).<sup>18</sup> The results of Raman spectroscopy and <sup>13</sup>C DP MAS NMR show that most of the carbon is sp<sup>2</sup>-hybridized and polyaromatic in nature (Figures S3 and S5). As such, the functional groups present would have to be positioned around the periphery or defect sites of the carbon structure, and they have to be in the same plane as the graphene sheets.<sup>29,48</sup>

Upon chemical treatment, changes in the intensity ratio of characteristic peaks in the Raman spectra indicated increasing disorder of the carbon structures (Table 1), which is attributed to a lower degree of graphitization. The disorder of the carbon sheets is attributed to the formation of additional edges,<sup>40</sup> suggesting that there are more defects/cavities and exposed edges. The increased disorder of acidified samples is in agreement with a previous study that found that treatment with H<sub>2</sub>SO<sub>4</sub> etches and exfoliates the stacks of graphene sheets, creating more edges and cavities.<sup>29</sup> HWT acidified carbon had the same degree of graphitization as acidified carbon, indicating that hot liquid water treatment at 200 °C does not affect the order of the carbon structures.

There were no significant changes in the pore size distribution of the catalysts in the microporous range (Figure 1A). In the mesoporous range, acidified and reacidified carbon have a lower contribution of pore volume at around 3.8 nm, and this is probably due to the exfoliation of the carbon structure during acidification.<sup>49</sup> However, HWT acidified

carbon had the same pore size distribution as as-received carbon.

It was shown that treatment with hot liquid water at 200 °C is able to impart a small concentration of weak functional groups,<sup>28</sup> and this effect was also observed in this study (Table 2). As-received carbon possessed a small concentration of weak functional groups such as phenol, lactone, and carboxylic acid groups (Tables 2 and S4). After acidification, the concentration of acid sites increased significantly with a fraction of 0.42 being sulfonic acid groups. The initial treatment with hot liquid water in the synthesis of HWT acidified carbon imparts a small concentration of weak acid sites.<sup>28</sup> This is probably due to the increased self-ionization of water at higher temperatures,<sup>50</sup> allowing more hydronium ions to functionalize the carbon structure. It is assumed that the carbon sheets are susceptible to electrophilic attack by the hydronium ion due to pyramidalization and  $\pi$  misalignment that is present at the edges and curvatures of the sheet walls.<sup>51</sup> This reduces the number of active sites for functionalization in the subsequent acidification step, resulting in a lower fraction of sulfonic acid groups present. In the case of reacidified carbon, the second step of acidification resulted in a lower concentration of phenol groups but higher concentrations of lactone and carboxylic acid groups (Table S4), suggesting that the sample underwent oxidation by sulfuric acid. The resulting lower concentration of sulfonic acid groups could indicate that these functional groups are not stable in the second acidification step, allowing more of the edges of the carbon to be functionalized by weak acid groups.

During the continuous reactivity studies (Figures 2 and 3), the conversion of cellobiose and glucose reached a steady state within a short time, and no deactivation was observed during 11 h on stream. This indicates that the functional groups and the carbon structure are active and stable during reaction up to 200 °C. Note that these results are far less ambiguous than catalyst recycle experiments in batch reactors.

**Adsorption of Glucose and Cellobiose.** The adsorption of glucans plays a critical role in the catalytic performance of carbon catalysts. Studies have shown that adsorption occurs on the hydrophobic carbon surface and that hydrophilic functional groups have limited involvement.<sup>29,52,53</sup> Specifically, interactions between the CH groups of the adsorbates and the polyaromatic rings of the carbon surface are responsible for driving the adsorption process.<sup>54,55</sup> In addition, these CH- $\pi$  interactions are significantly stronger compared to interactions between the glucan chains.<sup>53</sup>

Adsorption isotherms in this study show that as-received carbon readily adsorbs both glucose and cellobiose (Table 4). Our results are in agreement with the literature in showing that van der Waals forces are dominant in the interactions between the CH groups of the adsorbates and the polyaromatic rings of the carbon surface.<sup>52–56</sup> This explains the large increase of the adsorption coefficient for cellobiose, as it possesses more CH groups compared to those of glucose.

For the chemically treated materials, the adsorption coefficient of glucose and cellobiose decreased by about 65% and 40%, respectively, compared to that of the as-received carbon. The decrease can be explained by competitive adsorption with water molecules as the surface becomes more hydrophilic due to the presence of functional groups. However, the adsorption process is still dominated by van der Waals forces as indicated by the relatively small changes in the energy terms that describe these interactions. Specifically, the decrease of the adsorption coefficient of cellobiose was less pronounced

than that of glucose, which possesses a smaller number of CH-groups that can interact with the surface. This translates to a difference in the free energy of adsorption ( $\Delta\Delta G$ ) between the sorbates of about 0.3 kcal/mol, which is small compared to adsorptions associated with chemisorption ( $>9.5$  kcal/mol) or the strength of a hydrogen bond (1.6 kcal/mol–4.8 kcal/mol).<sup>57</sup> Hence, functional groups are not involved in the adsorption process for the acidified materials.

It is suggested that  $\Delta\Delta G$  is also dependent on the degree of contact at the molecular level, between the carbon surface and adsorbate.<sup>29,52</sup> This refers to the extent of overlap between the polyaromatic carbon surface and the adsorbed glucans. Thus, the defect sites created in the acidification process are expected to favor the adsorption of cellobiose over glucose.

For the adsorption of glucose on the chemically treated materials, there was an increase in maximum uptake compared to that of the as-received carbon. However, the maximum uptake did not change significantly for the adsorption of cellobiose. It is speculated that the presence of defect sites and functional groups causes rotation of adsorbed glucose to adsorb in a more tightly packed manner.

**Effect of Strong and Weak Acid Sites in the Hydrolysis of Cellobiose.** It has been demonstrated that even weak acid sites on carbon can be active for the hydrolysis of cellulose and xylan.<sup>15,24,29</sup> Chung et al. recommended the use of weak acid sites because strong acid sites could leach into the aqueous solution during hydrolysis as they are less hydrothermally stable.<sup>24</sup> Furthermore, these acid sites could undergo ion exchange in the presence of dissolved aqueous salts. In another study, it was reported that an increased loading of Ru on mesoporous carbon (CMK-3) resulted in a small increase of glucose yield and a large increase in the yield of byproducts.<sup>58</sup> It was hypothesized that the Ru species formed strong acid sites that resulted in sequential side degradation reactions.

At steady state, the hydrolysis of cellobiose over as-received carbon yielded 21% conversion and 43% glucose selectivity (Table 2). It is not entirely surprising that this result is almost identical to the reaction in the absence of any catalyst, as the untreated carbon possessed only a small concentration of functional groups. On the basis of previous studies, it is expected that a certain amount of cellobiose is converted to glycosyl-fructose and glucosyl-mannose under hydrothermal conditions ( $>200$  °C),<sup>9,10</sup> while a small amount of cellobiose is hydrolyzed to glucose. Note that similar experiments in batch reactors could lead to ambiguous results because some amount of reactants and products could remain adsorbed on the catalyst when the reaction is stopped and cooled down to room temperature. By using a flow reactor, the products formed are continuously removed to prevent accumulation and the formation of undesirable products, such as insoluble humins. In this way, the results obtained from a flow reactor are reliable and indicative of the catalyst's performance under the specified reaction condition. The steady state conversion and selectivity results in the limited variability of the rate constants obtained (Table 2). In agreement with previous suggestions,<sup>35,36</sup> linear decay profiles showed that the reactions are first order in cellobiose and glucose, respectively (Figure S9). Note that the surface chemistry and kinetics obtained in this study can be extrapolated to reactors that could be used on an industrial scale.

The glucose selectivity over acidified carbon was similar to that of as-received carbon, but it had a higher conversion of 50% (Table 2). This indicates that the enhanced catalytic



activity is due to the presence of the additional functional groups, especially the sulfonic acid group since these accounted for 42% of the total acid sites present. It was reported that after the hydrolysis of oligomers to monomeric glucose, the presence of an acid catalyst accelerated the isomerization of glucose to fructose, which could degrade to other products such as HMF, levulinic acid, formic acid, and acetic acid under hydrothermal conditions.<sup>4</sup> In addition, insoluble humins could be formed by different pathways.<sup>59</sup> Therefore, it is speculated that the strongly acidic sulfonic acid groups in acidified carbon increased the conversion of cellobiose. However, these strong acid sites also appear to catalyze the conversion of glucose monomers to other side products, resulting in the same glucose selectivity as that of untreated carbon.

Cellobiose hydrolysis over HWT acidified carbon and reacidified carbon exhibited a lower conversion of about 40% but a higher glucose selectivity of 60–63% (Table 2). This is a result of a higher reaction rate constant of cellobiose hydrolysis to glucose. Although the conversion of glucose was small in the absence of a catalyst (Figure 3), the limited thermal degradation suggests that the yield of glucose can be increased further by limiting the extent to which nonsurface reactions occur. This could be achieved with an improved design for a fixed bed reactor setup, in which the liquid streams are heated and cooled more rapidly. In addition, a lower reaction temperature (<200 °C) might reduce the formation of degradation products in the bulk solution. However, the rate of the desired catalytic reaction would also decrease. Therefore, it appears as if the design of highly selective catalysts is one of the most promising routes for achieving a high glucose selectivity.

Weak and moderate acid sites on carbon, such as phenols, lactones, and carboxylic acids, are located at the edges and defect sites of the carbon sheets.<sup>29</sup> These acid sites are active and could be selective in the hydrolysis of cellobiose to yield glucose. It was shown that these weaker acid sites are less accessible than sulfonic acid groups in polar solvents.<sup>60</sup> Therefore, it is suggested that glucose can easily interact with strong sulfonic acid groups leading to degradation reactions. In contrast, catalysts with weaker acid sites are expected to minimize such side reactions. The high selectivity of HWT acidified carbon and reacidified carbon can be explained by the presence of the low fraction of a sulfonic acid group. It was reported that maleic acid, which has a higher  $pK_a$  than sulfuric acid, is equally effective in hydrolyzing cellobiose but achieves higher glucose yields.<sup>61</sup> This further illustrates that under certain conditions (vide infra) the hydrolysis only requires relatively weak acid sites, whereas the extent of degradation of glucose increases in the presence of stronger acid sites, such as sulfonic acid groups. Further evidence for this scenario is the lower rate of glucose conversion over HWT acidified carbon compared to that of acidified carbon (Figure 3), which seems to indicate that the strength of acid sites is crucial for glucose selectivity in the hydrolysis of cellobiose. Consequently, a higher glucose yield is achieved when there are fewer sulfonic acid groups present on the carbon surface. In addition, a higher concentration of weaker acid sites (carboxylic acid, lactone, and phenol) improves the selectivity of the hydrolysis of cellobiose to glucose.

A previous study showed that the presence of defect sites can enhance the catalytic activity of activated carbon in the hydrolysis of cellulose.<sup>29</sup> It was hypothesized that the adsorption of oligomers on defect sites or edges of the carbon

structure induces a conformational change.<sup>3</sup> This allows the exposed glycosidic bond to be attacked by the in-plane functional groups, allowing weak acid sites to participate in the hydrolysis reaction. In the present study, all of the chemically treated materials have a lower degree of graphitization due to acidification and exfoliation compared to that of as-received carbon, and the functional groups are also located around the edges and defect sites of the carbon structure (vide supra). Furthermore, the lower  $\Delta\Delta G$  values from adsorption isotherms indicate that adsorption of cellobiose is preferable over materials with defect sites. Thus, it is proposed that the same adsorption and reaction mechanism can also occur on these materials, allowing weaker acid sites to selectively hydrolyze cellobiose.

Adsorption isotherms show that the adsorption coefficient of glucose is small compared to that of cellobiose due to weaker van der Waals interactions. Since glucose monomers compete unfavorably with water and cellobiose in its adsorption on functionalized carbon materials during the hydrolysis reaction, the surface is mostly likely to be populated with cellobiose. Thus, it would be difficult for weak acid sites to further catalyze glucose into fructose and other side products. Furthermore, these weak acid sites have limited strength to catalyze these degradation reactions based on the lower rate of glucose conversion over HWT acidified carbon. This results in a higher and sustained selectivity of glucose at various W/F ratios. In addition, it is suggested that glucose can be degraded if a sulfonic acid group is within the vicinity when cellobiose is hydrolyzed, as sulfonic acid groups appear to be more accessible for glucose molecules in the presence of a polar solvent.<sup>60</sup> In summary, these considerations show that weak acid sites in specific environments (i.e., defect sites and edges) are sufficient to catalyze the hydrolysis of oligosaccharides, but degradation reactions are prevented due to the limited strength of these sites.

## CONCLUSIONS

This study examines the catalytic activity of activated carbon functionalized with different fractions of sulfonic acid groups and weak acid sites in the hydrolysis of cellobiose. All of the acidified materials have a lower degree of graphitization, and adsorption isotherms reveal that the adsorption of glucose and cellobiose is driven by van der Waals forces between the CH groups of the adsorbates and the polyaromatic ring surface of the carbon catalysts. Reactivity studies in a continuously operated packed bed reactor setup show that the catalysts retain their initial activity for at least 11 h on stream. A high fraction of sulfonic acid groups results in a high conversion of cellobiose and low selectivity of glucose, while the materials with a high fraction of weaker acid sites exhibit high glucose selectivity but lower conversion. It is proposed that high glucose selectivity requires a synergistic effect between defect sites of the carbon structure and in-plane functional groups, which only allows weak acid sites to selectively catalyze the hydrolysis of cellobiose. This is possible because glucose competes unfavorably with cellobiose, and these weak acid sites have limited strength to carry out the degradation reactions. The higher accessibility of strong sulfonic acid groups in the presence of a polar solvent can further catalyze glucose monomers into fructose and other side products. These surface interactions result in a constant glucose selectivity regardless of the residence time of the feed in the catalyst bed.

## ■ ASSOCIATED CONTENT

### ● Supporting Information

The Supporting Information is available free of charge on the ACS Publications website at DOI: 10.1021/acssuschemeng.5b00530.

Mass transfer limitation tests, Raman spectra, XRD patterns, <sup>13</sup>C DP MAS NMR spectra, pore surface areas, PIXE analysis, concentrations of weak acid sites, reactivity of carbon catalysts, adsorption isotherms, and validation of first order reaction. (PDF)

## ■ AUTHOR INFORMATION

### Corresponding Author

\*E-mail: carsten.sievers@chbe.gatech.edu.

### Notes

The authors declare no competing financial interest.

## ■ ACKNOWLEDGMENTS

The Renewable Bioproducts Institute is acknowledged for the use of its facilities. We thank Johannes Leisen for experimental assistance with <sup>13</sup>C DP MAS NMR. Funding from Renmatix, Inc. and the U.S. Department of Energy (grant DE-AC36-08-GO28308) is gratefully acknowledged.

## ■ REFERENCES

- (1) Huber, G. W.; Iborra, S.; Corma, A. Synthesis of transportation fuels from biomass: Chemistry, catalysts, and engineering. *Chem. Rev.* **2006**, *106*, 4044–4098.
- (2) Ragauskas, A. J.; Williams, C. K.; Davison, B. H.; Britovsek, G.; Cairney, J.; Eckert, C. A.; Frederick, W. J.; Hallett, J. P.; Leak, D. J.; Liotta, C. L.; Mielenz, J. R.; Murphy, R.; Templer, R.; Tschaplinski, T. The path forward for biofuels and biomaterials. *Science* **2006**, *311*, 484–489.
- (3) Loerbroks, C.; Rinaldi, R.; Thiel, W. The Electronic Nature of the 1,4-beta-Glycosidic Bond and Its Chemical Environment: DFT Insights into Cellulose Chemistry. *Chem.—Eur. J.* **2013**, *19*, 16282–16294.
- (4) Zakzeski, J.; Grisel, R. J. H.; Smit, A. T.; Weckhuysen, B. M. Solid Acid-Catalyzed Cellulose Hydrolysis Monitored by In Situ ATR-IR Spectroscopy. *ChemSusChem* **2012**, *5*, 430–437.
- (5) Onda, A.; Ochi, T.; Kajiyoshi, K.; Yanagisawa, K. A new chemical process for catalytic conversion Of D-glucose into lactic acid and gluconic acid. *Appl. Catal., A* **2008**, *343*, 49–54.
- (6) Bermejo-Deval, R.; Assary, R. S.; Nikolla, E.; Moliner, M.; Román-Leshkov, Y.; Hwang, S.-J.; Palsdottir, A.; Silverman, D.; Lobo, R. F.; Curtiss, L. A.; Davis, M. E. Metalloenzyme-like catalyzed isomerizations of sugars by Lewis acid zeolites. *Proc. Natl. Acad. Sci. U. S. A.* **2012**, *109*, 9727–9732.
- (7) Corma, A.; Iborra, S.; Velty, A. Chemical routes for the transformation of biomass into chemicals. *Chem. Rev.* **2007**, *107*, 2411–2502.
- (8) Mosier, N.; Wyman, C.; Dale, B.; Elander, R.; Lee, Y. Y.; Holtzapple, M.; Ladisch, M. Features of promising technologies for pretreatment of lignocellulosic biomass. *Bioresour. Technol.* **2005**, *96*, 673–686.
- (9) Yu, Y.; Shafie, Z. M.; Wu, H. Cellobiose Decomposition in Hot-Compressed Water: Importance of Isomerization Reactions. *Ind. Eng. Chem. Res.* **2013**, *52*, 17006–17014.
- (10) Mohd Shafie, Z.; Yu, Y.; Wu, H. Insights into the Primary Decomposition Mechanism of Cellobiose under Hydrothermal Conditions. *Ind. Eng. Chem. Res.* **2014**, *53*, 14607–14616.
- (11) Harris, E. E.; Beglinger, E.; Hajny, G. J.; Sherrard, E. C. Hydrolysis of Wood - Treatment with Sulfuric Acid in a Stationary Digester. *Ind. Eng. Chem.* **1945**, *37*, 12–23.

- (12) Sherrard, E. C.; Kressman, F. W. Review of Processes in the United States prior to World War II. *Ind. Eng. Chem.* **1945**, *37*, 5–8.

- (13) Harris, E. E.; Beglinger, E. Madison Wood Sugar Process. *Ind. Eng. Chem.* **1946**, *38*, 890–895.

- (14) Marzioletti, T.; Olarte, M. B. V.; Sievers, C.; Hoskins, T. J. C.; Agrawal, P. K.; Jones, C. W. Dilute acid hydrolysis of Loblolly pine: A comprehensive approach. *Ind. Eng. Chem. Res.* **2008**, *47*, 7131–7140.

- (15) Kobayashi, H.; Yabushita, M.; Komanoya, T.; Hara, K.; Fujita, I.; Fukuoka, A. High-Yielding One-Pot Synthesis of Glucose from Cellulose Using Simple Activated Carbons and Trace Hydrochloric Acid. *ACS Catal.* **2013**, *3*, 581–587.

- (16) Suganuma, S.; Nakajima, K.; Kitano, M.; Yamaguchi, D.; Kato, H.; Hayashi, S.; Hara, M. Hydrolysis of cellulose by amorphous carbon bearing SO<sub>3</sub>H, COOH, and OH groups. *J. Am. Chem. Soc.* **2008**, *130*, 12787–12793.

- (17) Kitano, M.; Yamaguchi, D.; Suganuma, S.; Nakajima, K.; Kato, H.; Hayashi, S.; Hara, M. Adsorption-Enhanced Hydrolysis of  $\beta$ -1,4-Glucan on Graphene-Based Amorphous Carbon Bearing SO<sub>3</sub>H, COOH, and OH Groups. *Langmuir* **2009**, *25*, 5068–5075.

- (18) Fukuhara, K.; Nakajima, K.; Kitano, M.; Kato, H.; Hayashi, S.; Hara, M. Structure and Catalysis of Cellulose-Derived Amorphous Carbon Bearing SO<sub>3</sub>H Groups. *ChemSusChem* **2011**, *4*, 778–784.

- (19) Nakajima, K.; Hara, M. Amorphous Carbon with SO<sub>3</sub>H Groups as a Solid Bronsted Acid Catalyst. *ACS Catal.* **2012**, *2*, 1296–1304.

- (20) Onda, A. Selective Hydrolysis of Cellulose and Polysaccharides into Sugars by Catalytic Hydrothermal Method Using Sulfonated Activated-carbon. *J. Jpn. Pet. Inst.* **2012**, *55*, 73–86.

- (21) Huang, Y.-B.; Fu, Y. Hydrolysis of cellulose to glucose by solid acid catalysts. *Green Chem.* **2013**, *15*, 1095–1111.

- (22) Pang, J. F.; Wang, A. Q.; Zheng, M. Y.; Zhang, T. Hydrolysis of cellulose into glucose over carbons sulfonated at elevated temperatures. *Chem. Commun.* **2010**, *46*, 6935–6937.

- (23) Torget, R. W.; Kim, J. S.; Lee, Y. Y. Fundamental Aspects of Dilute Acid Hydrolysis/Fractionation Kinetics of Hardwood Carbohydrates. 1. Cellulose Hydrolysis. *Ind. Eng. Chem. Res.* **2000**, *39*, 2817–2825.

- (24) Chung, P.-W.; Charmot, A.; Olatunji-Ojo, O. A.; Durkin, K. A.; Katz, A. Hydrolysis Catalysis of Miscanthus Xylan to Xylose Using Weak-Acid Surface Sites. *ACS Catal.* **2014**, *4*, 302–310.

- (25) Gazit, O. M.; Charmot, A.; Katz, A. Grafted cellulose strands on the surface of silica: effect of environment on reactivity. *Chem. Commun.* **2011**, *47*, 376–378.

- (26) Gazit, O. M.; Katz, A. Grafted Poly(1  $\rightarrow$  4-beta-glucan) Strands on Silica: A Comparative Study of Surface Reactivity as a Function of Grafting Density. *Langmuir* **2012**, *28*, 431–437.

- (27) Gazit, O. M.; Katz, A. Understanding the Role of Defect Sites in Glucan Hydrolysis on Surfaces. *J. Am. Chem. Soc.* **2013**, *135*, 4398–4402.

- (28) Van Pelt, A. H.; Simakova, O. A.; Schimming, S. M.; Ewbank, J. L.; Foo, G. S.; Pidko, E. A.; Hensen, E. J. M.; Sievers, C. Stability of functionalized activated carbon in hot liquid water. *Carbon* **2014**, *77*, 143–154.

- (29) Foo, G. S.; Sievers, C. Synergistic Effect between Defect Sites and Functional Groups on the Hydrolysis of Cellulose over Activated Carbon. *ChemSusChem* **2015**, *8*, 534–543.

- (30) Brunauer, S.; Emmett, P. H.; Teller, E. Adsorption of gases in multimolecular layers. *J. Am. Chem. Soc.* **1938**, *60*, 309–319.

- (31) Barrett, E. P.; Joyner, L. G.; Halenda, P. P. The determination of pore volume and area distributions in porous substances 0.1. Computations from nitrogen isotherms. *J. Am. Chem. Soc.* **1951**, *73*, 373–380.

- (32) Lastoskie, C.; Gubbins, K. E.; Quirke, N. Pore-Size Distribution Analysis of Microporous Carbons - A Density-Functional Theory Approach. *J. Phys. Chem.* **1993**, *97*, 4786–4796.

- (33) Oickle, A. M.; Goertzen, S. L.; Hopper, K. R.; Abdalla, Y. O.; Andreas, H. A. Standardization of the Boehm titration: Part II. Method of agitation, effect of filtering and dilute titrant. *Carbon* **2010**, *48*, 3313–3322.



- (34) Goertzen, S. L.; Theriault, K. D.; Oickle, A. M.; Tarasuk, A. C.; Andreas, H. A. Standardization of the Boehm titration. Part I. CO<sub>2</sub> expulsion and endpoint determination. *Carbon* **2010**, *48*, 1252–1261.
- (35) Xiang, Q.; Lee, Y. Y.; Pettersson, P. O.; Torget, R. Heterogeneous aspects of acid hydrolysis of alpha-cellulose. *Appl. Biochem. Biotechnol.* **2003**, *107*, 505–514.
- (36) Suib, S. L. *New and Future Developments in Catalysis: Catalytic Biomass Conversion*; Elsevier Science: New York, 2013.
- (37) Ferrari, A. C.; Robertson, J. Interpretation of Raman spectra of disordered and amorphous carbon. *Phys. Rev. B: Condens. Matter Mater. Phys.* **2000**, *61*, 14095–14107.
- (38) Prawer, S.; Nugent, K. W.; Jamieson, D. N.; Orwa, J. O.; Bursill, L. A.; Peng, J. L. The Raman spectrum of nanocrystalline diamond. *Chem. Phys. Lett.* **2000**, *332*, 93–97.
- (39) Sadezky, A.; Muckenhuber, H.; Grothe, H.; Niessner, R.; Poschl, U. Raman micro spectroscopy of soot and related carbonaceous materials: Spectral analysis and structural information. *Carbon* **2005**, *43*, 1731–1742.
- (40) Lezanska, M.; Pietrzyk, P.; Sojka, Z. Investigations into the Structure of Nitrogen-Containing CMK-3 and OCM-0.75 Carbon Replicas and the Nature of Surface Functional Groups by Spectroscopic and Sorption Techniques. *J. Phys. Chem. C* **2010**, *114*, 1208–1216.
- (41) Babu, V. S.; Seehra, M. S. Modeling of disorder and X-ray diffraction in coal-based graphitic carbons. *Carbon* **1996**, *34*, 1259–1265.
- (42) Manivannan, A.; Chirila, M.; Giles, N. C.; Seehra, M. S. Microstructure, dangling bonds and impurities in activated carbons. *Carbon* **1999**, *37*, 1741–1747.
- (43) Manoj, B.; Kunjomana, A. G. Study of Stacking Structure of Amorphous Carbon by X-Ray Diffraction Technique. *Int. J. Electrochem. Sci.* **2012**, *7*, 3127–3134.
- (44) Li, Z. Q.; Lu, C. J.; Xia, Z. P.; Zhou, Y.; Luo, Z. X-ray diffraction patterns of graphite and turbostratic carbon. *Carbon* **2007**, *45*, 1686–1695.
- (45) Cheng, H. N.; Wartelle, L. H.; Klasson, K. T.; Edwards, J. C. Solid-state NMR and ESR studies of activated carbons produced from pecan shells. *Carbon* **2010**, *48*, 2455–2469.
- (46) Knicker, H.; Totsche, K. U.; Almendros, G.; Gonzalez-Vila, F. J. Condensation degree of burnt peat and plant residues and the reliability of solid-state VACP MAS C-13 NMR spectra obtained from pyrogenic humic material. *Org. Geochem.* **2005**, *36*, 1359–1377.
- (47) Lennon, D.; Lundie, D. T.; Jackson, S. D.; Kelly, G. J.; Parker, S. F. Characterization of activated carbon using X-ray photoelectron spectroscopy and inelastic neutron scattering spectroscopy. *Langmuir* **2002**, *18*, 4667–4673.
- (48) Boehm, H. P. Some aspects of the surface chemistry of carbon blacks and other carbons. *Carbon* **1994**, *32*, 759–769.
- (49) Hong, Y.; Wang, Z.; Jin, X. Sulfuric acid intercalated graphite oxide for graphene preparation. *Sci. Rep.* **2013**, *3*. [10.1038/srep03439](https://doi.org/10.1038/srep03439)
- (50) Pitzer, K. S. Self-Ionization of Water at High-Temperature and the Thermodynamic Properties of Properties of the Ions. *J. Phys. Chem.* **1982**, *86*, 4704–4708.
- (51) Quinlan, R. A. The Functionalization of Carbon Nanosheets. Ph.D. Dissertation, College of William and Mary, Williamsburg, VA, 2009.
- (52) Chung, P.-W.; Charmot, A.; Gazit, O. M.; Katz, A. Glucan Adsorption on Mesoporous Carbon Nanoparticles: Effect of Chain Length and Internal Surface. *Langmuir* **2012**, *28*, 15222–15232.
- (53) Yabushita, M.; Kobayashi, H.; Hasegawa, J.-y.; Hara, K.; Fukuoka, A. Entropically Favored Adsorption of Cellulosic Molecules onto Carbon Materials through Hydrophobic Functionalities. *ChemSusChem* **2014**, *7*, 1443–1450.
- (54) Kiehna, S. E.; Laughrey, Z. R.; Waters, M. L. Evaluation of a carbohydrate-pi interaction in a peptide model system. *Chem. Commun.* **2007**, 4026–4028.
- (55) Laughrey, Z. R.; Kiehna, S. E.; Riemen, A. J.; Waters, M. L. Carbohydrate- $\pi$  Interactions: What Are They Worth? *J. Am. Chem. Soc.* **2008**, *130*, 14625–14633.
- (56) Chinn, D.; King, C. J. Adsorption of glycols, sugars, and related multiple -OH compounds onto activated carbons. 1. Adsorption mechanisms. *Ind. Eng. Chem. Res.* **1999**, *38*, 3738–3745.
- (57) Sheu, S. Y.; Yang, D. Y.; Selzle, H. L.; Schlag, E. W. Energetics of hydrogen bonds in peptides. *Proc. Natl. Acad. Sci. U. S. A.* **2003**, *100*, 12683–12687.
- (58) Kobayashi, H.; Ohta, H.; Fukuoka, A. Conversion of lignocellulose into renewable chemicals by heterogeneous catalysis. *Catal. Sci. Technol.* **2012**, *2*, 869–883.
- (59) Sievers, C.; Musin, I.; Marzioletti, T.; Olarte, M. B. V.; Agrawal, P. K.; Jones, C. W. Acid-Catalyzed Conversion of Sugars and Furfurals in an Ionic-Liquid Phase. *ChemSusChem* **2009**, *2*, 665–671.
- (60) Fraile, J. M.; García-Bordejé, E.; Pires, E.; Roldán, L. New insights into the strength and accessibility of acid sites of sulfonated hydrothermal carbon. *Carbon* **2014**, *77*, 1157–1167.
- (61) Mosier, N. S.; Sarikaya, A.; Ladisch, C. M.; Ladisch, M. R. Characterization of dicarboxylic acids for cellulose hydrolysis. *Biotechnol. Prog.* **2001**, *17*, 474–480.